

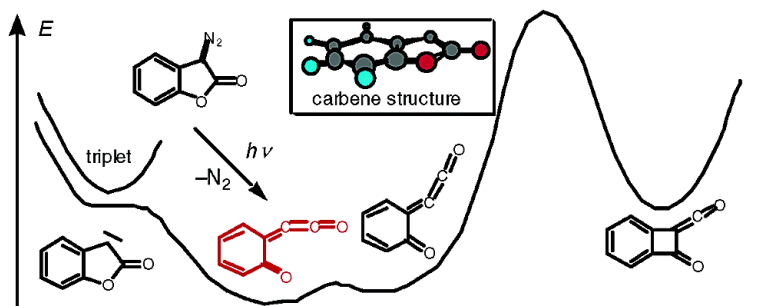
Article

Photoreactions of 3-Diazo-3*H*-benzofuran-2-one; Dimerization and Hydrolysis of Its Primary Photoproduct, A Quinonoid Cumulenone: A Study by Time-Resolved Optical and Infrared Spectroscopy

Yvonne Chiang, Martin Gaplovsky, A. Jerry Kresge, King Hung Leung, Christian Ley, Marek Mac, Gabriele Persy, David L. Phillips, Vladimir V. Popik, Christoph Rdig, Jakob Wirz, and Yu Zhu

J. Am. Chem. Soc., **2003**, 125 (42), 12872-12880 • DOI: 10.1021/ja0365476 • Publication Date (Web): 27 September 2003

Downloaded from <http://pubs.acs.org> on March 30, 2009



More About This Article

Additional resources and features associated with this article are available within the HTML version:

- Supporting Information
- Access to high resolution figures
- Links to articles and content related to this article
- Copyright permission to reproduce figures and/or text from this article

[View the Full Text HTML](#)

Photoreactions of 3-Diazo-3*H*-benzofuran-2-one; Dimerization and Hydrolysis of Its Primary Photoproduct, A Quinonoid Cumulenone: A Study by Time-Resolved Optical and Infrared Spectroscopy

Yvonne Chiang,[†] Martin Gaplovsky,[‡] A. Jerry Kresge,^{*,†} King Hung Leung,[§]
Christian Ley,[‡] Marek Mac,[‡] Gabriele Persy,[‡] David L. Phillips,[§] Vladimir V. Popik,^{†,||}
Christoph Rödig,[‡] Jakob Wirz,^{*,‡} and Yu Zhu[†]

Contribution from The Department of Chemistry, University of Toronto, Toronto, Ontario M5S 3H6, Canada, Departement Chemie, Universität Basel, Klingelbergstrasse 80, CH-4056 Basel, Switzerland, and the Department of Chemistry, University of Hong Kong, Pokfulham Road, Hong Kong S.A.R., P.R China

Received June 6, 2003

Abstract: Light-induced deazotization of 3-diazo-3*H*-benzofuran-2-one (**1**) in solution is accompanied by facile (CO)–O bond cleavage yielding 6-(oxoethenylidene)-2,4-cyclohexadien-1-one (**3**), which appears with a rise time of 28 ps. The expected Wolff-rearrangement product, 7-oxabicyclo[4.2.0]octa-1,3,5-trien-8-ylidenemethanone (**4**), is not formed. The efficient light-induced formation of the quinonoid cumulenone **3** opens the way to determine the reactivity of a cumulenone in solution. The reaction kinetics of **3** were monitored by nanosecond flash photolysis with optical ($\lambda_{\text{max}} \approx 460$ nm) as well as Raman (1526 cm^{-1}) and IR detection (2050 cm^{-1}). Remarkably, the reactivity of **3** is that expected from its valence isomer, the cyclic carbene 3*H*-benzofuran-2-one-3-ylidene, **2**. In aqueous solution, acid-catalyzed addition of water forms the lactone 3-hydroxy-3*H*-benzofuran-2-one (**5**). The reaction is initiated by protonation of the cumulenone on its β -carbon atom. In hexane, cumulenone **3** dimerizes to isoxindigo ((*E*)-[3,3']bibenzofuranylidene-2,2'-dione, **7**), coumestan (6*H*-benzofuro[3,2-*c*][1]benzopyran-6-one, **8**), and a small amount of dibenzonaphthyrone ([1]benzopyrano[4,3-*j*][1]benzopyran-5,11-dione, **9**) at a nearly diffusion-controlled rate. Ab initio calculations (G3) are consistent with the observed data. Carbene **2** is predicted to have a singlet ground state, which undergoes very facile, strongly exothermic (irreversible) ring opening to the cumulenone **3**. The calculated barrier to formation of **4** (Wolff-rearrangement) is prohibitive. DFT calculations indicate that protonation of **3** on the β -carbon is accompanied by cyclization to the protonated carbene 2H^+ , and that dimerization of **3** to **7** and **9** takes place in a single step with negligible activation energy.

Introduction

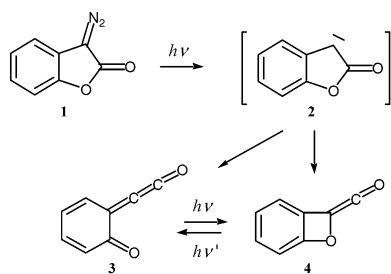
In 1902, Wolff¹ discovered the rearrangement of α -diazo-carbonyl compounds, which at the time were thought to have a cyclic 1,2,3-oxadiazole structure, to ketenes. In recent years, several α -carbonylcarbenes have been identified as transient intermediates in the photoinduced Wolff rearrangement,^{2–4} and

ab initio calculations have predicted substantial (10–75 kJ mol^{-1}) barriers to Wolff rearrangement of the singlet carbonyl carbenes showing some correlation with the exothermicity of ketene formation.⁵ In cases where the migratory aptitude of the potentially migrating group is poor, the Wolff rearrangement has been found to give way, in aqueous solution, to conjugate addition of water, forming β -hydroxyenol products.⁶

The α -carbonylcarbene **2** formed by dediazotization of 3-diazo-3*H*-benzofuran-2-one (**1**) has two options for further intramolecular reaction: (CO)–O ring cleavage to the quinonoid cumulenone **3**, and Wolff-rearrangement to the cyclic ketene **4**

- [†] University of Toronto. E-mail: AKresge@chem.utoronto.ca.
[‡] University of Basel. E-mail: J.Wirz@unibas.ch.
[§] University of Hong Kong. E-mail: Phillips@hkucc.hku.hk.
^{||} Present address: Department of Chemistry, Bowling Green State University, Bowling Green, OH. E-mail: VPopik@bgnnet.bgsu.edu.
(1) Wolff, L. *Justus Liebigs Ann. Chem.* **1902**, 325, 129–195.
(2) Bucher, G.; Scaiano, J. C.; Platz, M. S. *Kinetics of Carbene Reactions in Solution*, Landolt-Börnstein, Group II, Vol. 18, Subvolume E2; Springer: Germany, 1998; p 141. Toscano, J. P. In *Advances in Carbene Chemistry*; Brinker, U. H., Ed.; JAI Press: Greenwich, CT, 1998; Vol. 2, p 215.
(3) Toscano, J. P.; Platz, M. S.; Nikolaev, V.; Cao, Y.; Zimmt, M. B. *J. Am. Chem. Soc.* **1996**, 118, 3527–3528. Zhu, Z.; Bally, T.; Stracener, L. L.; McMahon, R. J. *J. Am. Chem. Soc.* **1999**, 121, 2863–2874. Wang, Y.; Hadad, C. M.; Toscano, J. P. *J. Am. Chem. Soc.* **1999**, 121, 2875–2882. Wang, Y.; Toscano, J. P. *J. Am. Chem. Soc.* **2000**, 122, 4512–4513. Wang, Y.; Hadad, C. M.; Toscano, J. P. *J. Am. Chem. Soc.* **2002**, 124, 1761–1767.
(4) Likhovorik, I.; Zhu, Z.; Tae, E. L.; Tippmann, E.; Hill, B. E.; Platz, M. S. *J. Am. Chem. Soc.* **2001**, 123, 6061–6068.

- (5) Scott, A. P.; Platz, M. S.; Radom, L. *J. Am. Chem. Soc.* **2001**, 123, 6069–6076.
(6) (a) Chiang, Y.; Kresge, A. J.; Popik, V. V.; Schepp, N. P. *J. Am. Chem. Soc.* **1997**, 119, 10 203–10 212. (b) Chiang, Y.; Jefferson, E. A.; Kresge, A. J.; Popik, V. V.; Xie, R.-Q. *J. Phys. Org. Chem.* **1998**, 11, 610–613. (c) Chiang, Y.; Eustace, S. J.; Jefferson, E. A.; Kresge, A. J.; Popik, V. V.; Xie, R.-Q. *J. Phys. Org. Chem.* **2000**, 13, 461–467. (d) Chiang, Y.; Kresge, A. J.; Schepp, N. P.; Xie, R.-Q. *J. Org. Chem.* **2000**, 65, 1175–1180. (e) Bakulev, V. A.; Chiang, Y.; Kresge, A. J.; Meng, Q.; Morzherin, Y. Y.; Popik, V. V. *J. Am. Chem. Soc.* **2001**, 123, 2681–2682. (f) Chiang, Y.; Guo, H.-X.; Kresge, A. J.; Richard, J. P.; Toth, K. *J. Am. Chem. Soc.* **2003**, 125, 187–194.

Scheme 1. Photoreactions of **1** in an Argon Matrix as Proposed by Chapman et al.⁷

(Scheme 1). In 1975, Chapman and co-workers⁷ studied the photoreactions of 3-diazo-3H-benzofuran-2-one (**1**) under matrix isolation conditions and identified both **3** and **4** as photochemical products. The presumed carbene intermediate **2** was not observed. Both **3** and **4** were stable at 12 K, but interconverted upon further irradiation, with short wavelength (254 nm) favoring **3**, and long wavelengths (>350 nm) favoring **4**. Soon after, Voigt and Meier⁸ reported formation of 2-(2-hydroxyphenyl)-2-methoxyacetic acid methyl ester upon irradiation of **1** in methanol solution. These authors considered several reaction paths and concluded that the reaction proceeds either by direct O–H insertion of the carbene **2** into methanol or via the cyclic ketene **4**.

We have studied the photoreaction of **1** in solution by time-resolved optical, infrared and Raman spectroscopy. We identify cumulenone **3** as the sole primary photoproduct of **1** in solution, and report on its reaction kinetics in aqueous acid and in aprotic solvents. A kinetic investigation of the thermal, acid-catalyzed hydrolysis of **1** to 3-hydroxy-3H-benzofuran-2-one (**5**), and further hydrolysis of **5** to 2-hydroxymandelic acid (**6**), was reported in a separate paper.⁹

Experimental Section

Materials. 3-Diazo-3H-benzofuran-2-one (**1**) was synthesized from isatin (2,3-indolinedione, Aldrich) by the route described¹⁰ with some modification of the experimental details (cf. Supporting Information).¹¹ 3-Hydroxy-3H-benzofuran-2-one (**5**) and 2-hydroxymandelic acid (**6**) were samples that had been prepared for another purpose.⁹ Solvents were of spectroscopic grade, where available. Genetron 113 (1,1,2-trichlorotrifluoroethane) was purchased from Fluka.

Step-Scan IR. The design of the step-scan apparatus was that described in detail by Siebert and co-workers.¹² Solutions of **1** in mixtures of CD₃CN and D₂O were pumped through a sample cell (CaF₂) with either a peristaltic pump (Ismatec MS-2/12–160) or a graphite cog-wheel pump (Ismatec Reglo-Z). The temperature in the sample chamber of the instrument was about 30 °C. Solute concentrations were adjusted to an absorbance of 0.5 (200 μm path length) at the excitation wavelength. A Quantel Brillant W Q-switched Nd:YAG laser operated at 10 Hz was used for excitation. The frequency-quadrupled (266 nm) pulses of 4.3 ns duration (fwhm) were reduced to about 6 mJ per pulse and the pulse diameter was widened to 8 mm at the sample. The spectra

were collected on a Bruker IFS 66 v/S Fourier transform instrument. An IR-band-pass filter (2257–1129 cm⁻¹) was inserted between the probe and the interferometer. The signals from a photovoltaic MCT detector (Kolmar 100–1-B) were processed by a 20-MHz dc-coupled preamplifier (Kolmar KA020-E6/MU), and further by a home-built amplifier with a rise time of 20 ns at 200-fold amplification. This setup had a rise time of 50 ns. To reduce noise, the signals were usually passed through an electronic low-pass filter, which increased the rise time to 330 ns. The signals were fed to a 50-Ohm load on the transient recorder (Spectrum, PAD 1232, maximum sampling rate 40 MHz).

Time-Resolved Raman Spectroscopy. The experimental setup has been described previously¹³ so only a brief description is given here. Solutions of **1** were prepared in either pure acetonitrile or mixed water/acetonitrile (50%/50 vol %) solvent. The fourth harmonic (266 nm) and the first anti-Stokes hydrogen Raman shifted laser line (436 nm) of the second harmonic from a Nd:YAG laser provided the pump and probe excitation wavelengths, respectively. An optical delay of about 10 ns between the pump and probe pulses was used in the experiments. The pump and probe beams were lightly focused onto a flowing liquid stream of sample solution using a near collinear geometry. The Raman scattering was acquired using a backscattering geometry and reflective optics and imaged through a depolarizer mounted on the entrance slit of a 0.5-meter spectrograph. The Raman light was then dispersed onto a CCD detector and accumulated for about 300 to 600 s before being read out to an interfaced PC computer and 10 to 20 read outs were added together to obtain a resonance Raman spectrum. Pump only, probe only, and pump–probe Raman spectra as well as a background scan were acquired. The known Raman bands of the acetonitrile and water/acetonitrile solvents were used to calibrate the Raman shifts of the spectra. The solvent and precursor **1** Raman bands were removed from the pump–probe transient resonance Raman spectrum by subtracting a probe only Raman spectrum. The pump only spectrum and a background scan were also subtracted from the pump–probe spectrum so as to obtain the transient resonance Raman spectrum.

Laser Flash Photolysis (LFP). Measurements with acidic aqueous solutions were made using an excimer laser nanosecond flash photolysis system (Toronto) that provided a 20-ns, 100-mJ, 248-nm pulse. The sample temperature was controlled at 25.0 ± 0.1 °C. Transient decays conformed to the first-order rate law well, and observed first-order rate constants were obtained by nonlinear least-squares fitting of an exponential function. LFP of **1** in aprotic solvents was done with a similar setup (Basel).

Product Analyses. Product compositions formed by irradiation of **1** in acidic aqueous solution were determined by HPLC using a Varian Vista 5500 instrument with a NovoPak C₁₈ reverse phase column and methanol–water (70:30) as the eluent. Reaction solutions containing the photolysis substrate at the same concentration as used for flash photolysis (10⁻⁴ M) were subjected to three flashes from a microsecond flash photolysis system.¹⁴ Control experiments showed that the photolysis products formed by the first flash did not undergo further photoreactions in the subsequent two flashes. Products were identified by comparing retention times and UV spectra with those of authentic samples.

Calculations. All quantum chemical calculations were done with the Gaussian 98 package of programs.¹⁵ Geometries of stationary points (intermediates and transition states) were optimized using either B3LYP density functional theory or MP2 perturbation theory with the 6-31G-(d) basis set. Frequency calculations were done for all stationary points and the connection of the transition states with the reactants 2–4 was established by intrinsic reaction path (IRC) calculations. The standard G3(MP2)^{16a} composite procedure as well as its variant G3(MP2)//B3LYP^{5,16b} were used to calculate the energies of selected species.

(7) Chapman, O. L.; Chang, C.-C.; Kole, J.; Rosenquist, N. R.; Tomioka, H. *J. Am. Chem. Soc.* **1975**, *97*, 6586–6588.

(8) Voigt, E.; Meier, H. *Chem. Ber.* **1977**, *110*, 2242–2248.

(9) Chiang, Y.; Kresge, A. J.; Meng, Q. *Can. J. Chem.* **2002**, *80*, 82–88.

(10) (a) Horspool, W. M.; Khandelwal, G. D. *J. Chem. Soc. (C)* **1971**, 3328–3331. (b) Huntress, E. H.; Hearon, W. A. *J. Am. Chem. Soc.* **1941**, *63*, 2762–2766.

(11) Supporting Information: see paragraph at the end of this paper regarding availability.

(12) Uhmman, W.; Becker, A.; Taran, C.; Siebert, F. *Appl. Spectrosc.* **1991**, *45*, 390–397. Rödig, C.; Siebert, F. *Appl. Spectrosc.* **1999**, *53*, 893–901.

(13) Zhu, P.; Ong, S. Y.; Chan, P. Y.; Leung, K. H.; Phillips, D. L. *J. Am. Chem. Soc.* **2001**, *123*, 2645–2649.

(14) Chiang, Y.; Hojatti, M.; Keeffe, J. R.; Kresge, A. J.; Schepp, N. P.; Wirz, J. *J. Am. Chem. Soc.* **1987**, *109*, 4000–4009.

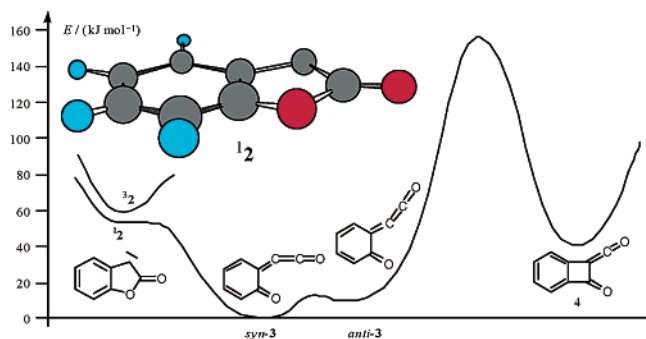


Figure 1. G3(MP2)//B3LYP zero-point energies (relative to *syn*-cumulenone **3**, Table 1) of the stationary points connecting **2**–**4**. The structure shown on top is that calculated for the singlet carbene **2**.

Table 1. Calculated Zero-Point Energies (relative to cumulenone **3**) of Reaction Intermediates **2**–**4** and the Transition States Connecting Them

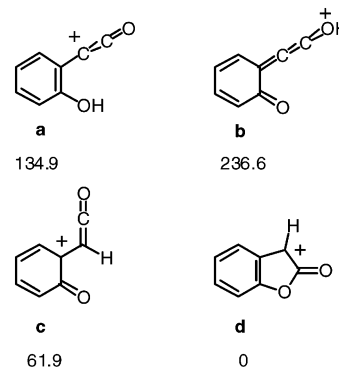
stationary points	$\Delta E / (\text{kJ mol}^{-1})$			
	B3LYP/6-31G(d)	MP2/6-31G(d)	G3MP2	G3MP2/B3LYP
12	61.4	74.8	54.2	54.5
32	42.8	162.0	60.0	59.4
<i>syn</i> - 3	0	0	0	0
<i>anti</i> - 3	12.2	16.7		13.0
4	45.9	43.0	41.5	42.6
12 → <i>syn</i> - 3 ^a	60.6 ^b	73.3 ^b		52.8
<i>syn</i> - 3 → 4 ^a	155.6	154.8		157.1
<i>syn</i> - 3 → <i>anti</i> - 3 ^a	12.7	22.7		15.2

Vibrational corrections were obtained from the corresponding frequency calculations, which were scaled by standard factors of 0.9804 for B3LYP, 0.9676 for MP2, 0.8929 for G3(MP2), and 0.96 for G3(MP2)//B3LYP.¹⁶ ^a Transition state. ^b The transition state energy was below that of **12** after zero-point energy correction.

Results

Calculations. The energies of the stationary points for intermediates **2**–**4** and the transition states connecting these species are depicted in Figure 1. The structures were optimized by the B3LYP/6-31G(d) method and the energies were recalculated by the G3(MP2)//B3LYP model. In a recent theoretical study,⁵ this high-level theory was found to give reliable results for singlet–triplet energy gaps of α -carbonylcarbenes and the energy barriers to Wolff-rearrangement. Compounds **2**–**4** were also calculated with the standard G3(MP2) model, which gave very similar results (Table 1). Both of these methods predict a singlet ground state for carbene **2** and a singlet–triplet energy gap of about 5 kJ mol⁻¹. The energy of the singlet carbene, **12**, is calculated to be 54 kJ mol⁻¹ above that of **3**. However, relative energies predicted for **12** and **32** by the B3LYP and MP2 methods differed quite substantially. Not surprisingly, high-level methods are required for an adequate treatment of these open-

Chart 1. Relative Calculated Energies^a in kJ mol⁻¹ for the Different Structures of Protonated Cumulenone **3**



^a Zero-point energies calculated by DFT (B3LYP/6-31G(d)). Frequencies were scaled by a factor of 0.9804. Absolute energies and structures are given in Table S4 of the Supporting Information.¹¹

shell species. On the other hand, the energies calculated for **3** and **4**, and for the transition states connecting them, showed satisfactory agreement between the four methods (Table 1). The cumulenone moiety of **3** is kinked, as are the parent cumulenones,¹⁷ and the “*syn*”-isomer was predicted to be about 13 kJ mol⁻¹ more stable than its “*anti*”-counterpart.

Ring cleavage of **12** to the cumulenone **3** encounters a negligible barrier. A stationary point with one imaginary frequency lying just a few kJ mol⁻¹ above **12** was located by both the MP2 and the B3LYP models. However, after correction for the zero-point energies, the energy of this point was slightly below that of **12**. On the other hand, a large barrier of about 156 kJ mol⁻¹ separates cumulenone **3** from ketene **4** and no other transition state could be located for the Wolff-rearrangement, **12** → **4**.

The dimerization of cumulenone **3** to give either isoxindigo (**7**) or dibenzonaphthyrone (**8**) was studied by DFT calculations using the B3LYP functional and the 6-31G(d) basis set. Both reactions are highly exothermic, ΔH (298 K) = -573 and -618 kJ mol⁻¹, respectively, and they also face a negligible barrier: A stationary point with one imaginary frequency (for the incipient bond between the β -sp carbon atoms on each cumulenone) was located which, however, had a zero-point energy 9 kJ mol⁻¹ lower than that of two separate molecules **3**. This may in part be attributed to the effect of basis set superposition. The calculated free energy of this stationary point (298 K) lies 46 kJ mol⁻¹ above that of two separate molecules due to the entropic contributions. Attempts to locate a stationary minimum for a diradical intermediate with a single bond connecting the two cumulenones failed. Optimization of such trial structures always led to one of the dimers **7** or **8**.

Finally, gas-phase DFT calculations (B3LYP) were done for the addition of a proton to the three conceivable protonation sites of cumulenone **3**. The results are shown in Chart 1. A stable minimum for protonation at the β -carbon of the cumulenone moiety, structure **c**, was found only when the calculation was started with the proton situated in plane and *endo* to the β -carbon atom. When the proton was initially placed *exo* to the β -carbon, optimization directly proceeded to the cyclic structure **d**, which corresponds to the protonated carbene **2**, and is the most stable of the carbocation structures **a**–**d**.

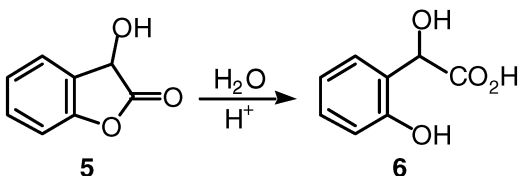
- (15) Frisch, M. J.; Trucks, G. W.; Schlegel, H. B.; Scuseria, G. E.; Robb, M. A.; Cheeseman, J. R.; Zakrzewski, V. G.; Montgomery, J. A.; Stratmann, R. E., Jr.; Burant, J. C.; Dapprich, S.; Millam, J. M.; Daniels, A. D.; Kudin, K. N.; Strain, M. C.; Farkas, O.; Tomasi, J.; Barone, V.; Cossi, M.; Cammi, R.; Mennucci, B.; Pomelli, C.; Adamo, C.; Clifford, S.; Ochterski, J.; Petersson, G. A.; Ayala, P. Y.; Cui, Q.; Morokuma, K.; Malick, D. K.; Rabuck, A. D.; Raghavachari, K.; Foresman, J. B.; Cioslowski, J.; Ortiz, J. V.; Stefanov, B. B.; Liu, G.; Liashenko, A.; Piskorz, P.; Komaromi, I.; Gomperts, R.; Martin, R. L.; Fox, D. J.; Keith, T.; Al-Laham, M. A.; Peng, C. Y.; Nanayakkara, A.; Gonzalez, C.; Challacombe, M.; Gill, P. M. W.; Johnson, B.; Chen, W.; Wong, M. W.; Andres, J. L.; Gonzalez, C.; Head-Gordon, M.; Replogle, E. S.; Pople, J. A. *GAUSSIAN 98*, Revision A.5; Gaussian, Inc.: Pittsburgh, PA, 1998.
- (16) (a) Curtiss, L. A.; Raghavachari, K.; Redfern, P. C.; Rassolov, V.; Pople, J. A. *J. Chem. Phys.* **1998**, *109*, 7764–7776. (b) Baboul, A. G.; Curtiss, L. A.; Redfern, P. C.; Raghavachari, K. *J. Chem. Phys.* **1999**, *110*, 7650–7657.

- (17) Scott, A. P.; Radom, L. *J. Mol. Struct.* **2000**, *556*, 253–261.

Table 2. Experimental Raman and IR Bands (cm^{-1}) with the Highest Intensities of Cumulenone **3**, and Calculated Bands (B3LYP/6-31G(d), Scaled with a Factor of 0.9613) for **2–4**

compd	2	3	4
IR exp		2050	2150 ^a
IR calc	1417 (112) 1598 (336) 1838 (212)	1725 (380) 1567 (85)	2083 (1291) 2146 (967)
Raman exp		2071 1618 1526 1402 1241	
Raman calcd	3107 (210) 3102 (106) 3089 (94) 3071 (92) 1838 (138)	1725 (174) 3086 (123) 3103 (246)	3100 (267) 3080 (119) 2084 (242) 1621 (78) 1590 (91) 1533.94 (411) 1418 (149) 1409 (81) 1164 (92) 1238 (80)

Calculated relative intensities are given in brackets. ^a From ref 7.

Scheme 2

Frequencies and IR- and Raman-intensities of the strongest vibrational transitions for the transient intermediates **3** and **4** and for the singlet and triplet states of carbene **2** calculated at the B3LYP/6-31G(d) level of theory are given in Table 2.

Product Analysis, Aqueous Solutions. HPLC analysis of photolyzed reaction mixtures obtained by flashing 10^{-3} and 10^{-5} M aqueous perchloric acid solutions of 3-diazo-3H-benzofuran-2-one (**1**), performed one minute after the flash, showed the presence of one major product, identified as 3-hydroxy-3H-benzofuran-2-one (**5**), plus minor amounts of 2-hydroxymandelic acid (**6**) and an additional unidentified substance. Subsequent analyses performed at longer times after flashing indicated that a further nonphotochemical reaction was converting **5** into **6** at a velocity consistent with the known rate of acid-catalyzed hydrolysis of this furanone to the substituted mandelic acid, Scheme 2.⁹ This subsequent reaction serves to reinforce identification of lactone **5** as the principal product formed by photolysis of **1** in acidic aqueous solution.

Product analyses were also performed on photolysis reaction mixtures formed by flashing 3-diazo-3H-benzofuran-2-one (**1**) in less acidic aqueous solutions, all the way up to 5×10^{-4} M sodium hydroxide. As these solutions became more basic, the yields of 3-hydroxy-3H-benzofuranon-2-one (**5**) and its hydrolysis product **6** decreased, and other unidentified products appeared. This increasing complexity discouraged us from examining the photochemistry of **1** in these more basic solutions in more detail.

Product Analysis, Hexane. Irradiation of **1** (16 mg) in hexane (50 mL) at 313 nm (medium-pressure mercury arc with band-pass filter) gave three major products that were separated by column chromatography using methylene chloride/hexane 1:1 as an eluent. The first, orange-red fraction was isoxindigo ((*E*)-[3,3']bibenzofuranylidene-2,2'-dione, **7**, 5 mg), which was identified by its characteristic ¹H NMR, UV/vis and mass

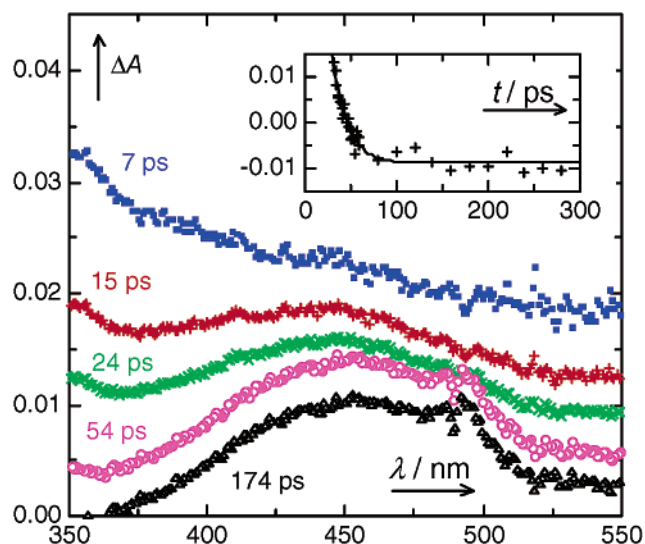


Figure 2. Picosecond pump–probe spectra of **1** in hexane. The kinks around 496 nm are artifacts due to the probe laser beam. The inset shows the loading coefficients of the second eigenvector determined by component analysis of 38 pump–probe spectra and a monoexponential fit function.

spectra.¹⁸ The second fraction (6 mg) contained mostly coumestan (6H-benzofuro[3,2-*c*][1]benzopyran-6-one, **8**),¹⁹ and a small amount of dibenzonaphthyrone ([1]benzopyrano[4,3-*c*][1]benzopyran-5,11-dione, **9**).¹⁸ The minor product **9** was identified in the second fraction by its characteristic absorption and fluorescence excitation and emission spectra,¹⁸ GC-MS, and the H NMR peaks at $\delta = 9.26$ ppm (dd, $J = 1.5$ and 8.4 Hz).¹⁸ Coumestan **8** was purified by sublimation at 130 °C in vacuo and identified by comparison with the H NMR, UV/Vis and mass spectral data given in the literature.¹⁹

Picosecond Pump–Probe Spectroscopy. Excitation of **1** in hexane at 248 nm with a subpicosecond pump pulse produced a structureless absorbance that decayed with a lifetime of 28 ps leaving a broad Gaussian absorption band, $\lambda_{\text{max}} = 460$ nm (Figure 2), which did not change further up to the maximum delay of 1.8 ns. Chapman et al.⁷ had observed the 460-nm band in their matrix work and attributed it to the quinonoid cumulenone **3**. This assignment will be corroborated below.

Nanosecond Laser Flash Photolysis (LFP). The transient absorption by **3**, $\lambda_{\text{max}} = 270$ and 460 nm, appeared within the duration of the laser pulse upon nanosecond LFP of **1** in Genetron 113 (1,1,2-trichlorotrifluoroethane) or in acetonitrile (Figure 3). It decayed by second-order kinetics and left persistent absorption at 460 nm. The addition of water (10% by vol) had little effect on the first half-life of **3** in acetonitrile, $\tau_{1/2} \approx 0.7$ ms, but the decay was accelerated, approaching first-order kinetics and leaving no end absorbance, upon addition of aqueous acid (upper inset of Figure 3). Because dimeric products (**7–9**) are formed by irradiation of **1** in aprotic solvents, the observed second-order rate law may be attributed to dimerization of **3**, $-dc_3/dt = 2kc_3^2$, where $c_3(t) = A_{450}(t)/[\epsilon_{450}(\mathbf{3})d]$ is the (unknown) concentration of transient **3** at time t after the laser pulse and $A_{450}(t)$ is the transient absorbance measured at 450 nm. Integration of this rate law gives $\tau_{1/2} = 1/[2kc_3(0)]$. The optical path length d of the sample cell was 4.2 cm. Assuming

(18) Becker, H.-D.; Lingnert, H. *J. Org. Chem.* **1982**, *47*, 1095–1101.

(19) Kraus, G. A.; Zhang, N. *J. Org. Chem.* **2000**, *65*, 6544–6546. Govindachari, T. R.; Nagarajan, K.; Parthasarathy, P. C. *J. Chem. Soc.* **1957**, 548–551.

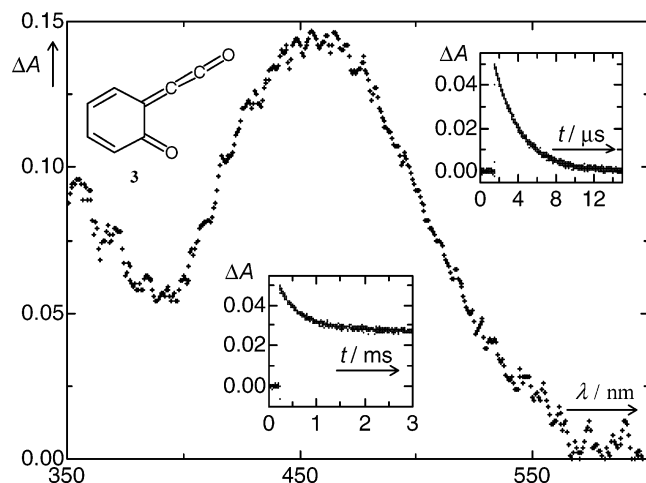


Figure 3. Spectrographic trace obtained by LFP of **1** in wet acetonitrile (10% water). The spectrum was recorded with a delay of 100 ns relative to the excitation pulse at 308 nm. The kinetic traces in the insets show the decay of transient absorbance at 450 nm in the same solvent mixture without (lower) and with (upper) addition of 1×10^{-3} M HClO_4 .

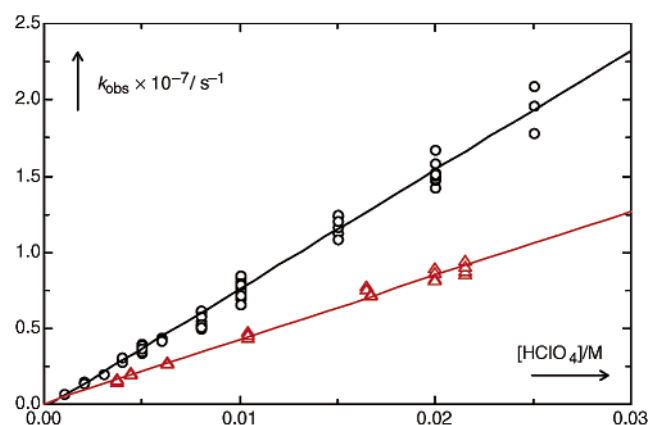


Figure 4. Observed decay rate constants of cumulenone **3** in H_2O (O) and D_2O (Δ) solutions at 25°C as a function of perchloric acid concentration (data in Table S1).¹¹

a molar absorbance coefficient $\epsilon_{450}(\mathbf{3}) \approx 5000 \text{ M}^{-1} \text{ cm}^{-1}$,²⁰ we estimate a value of $k \approx 3 \times 10^8 \text{ M}^{-1} \text{ s}^{-1}$ for the second-order rate constant of dimerization.

LFP of 3-diazo-3H-benzofuran-2-one (**1**) in acidic aqueous solution also produced intermediate **3**, $\lambda_{\text{max}} = 270$ and 460 nm , within the duration of the flash (20 ns). The transient decays were in the microsecond time range and obeyed the first-order rate law. Rates of decay were monitored at both $\lambda_{\text{max}} = 270$ and 460 nm and concordant results were obtained at the two wavelengths. These rates were measured in both H_2O and D_2O solutions of perchloric acid over the concentration range 0.001 – 0.025 M . The ionic strength of these solutions was maintained at 0.10 M by adding sodium perchlorate as required. The data so obtained are summarized in Table S1¹¹ and are displayed in Figure 4.

It may be seen that observed first-order rate constants increase linearly with increasing acid concentration. Linear regression produced the hydronium ion catalytic coefficient k_{H^+}

$= (7.45 \pm 0.08) \times 10^8 \text{ M}^{-1} \text{ s}^{-1}$ and the isotope effect $k_{\text{H}^+}/k_{\text{D}^+} = 1.74 \pm 0.03$.

Rates of transient decay were also measured in acetic acid buffer solutions. These measurements were made in series of solutions of varying buffer concentration but constant buffer ratio and constant ionic strength (0.10 M), and therefore constant hydronium ion concentration. The data so obtained are summarized in Table S2.¹¹

Within each of these buffer solution series, observed first-order rate constants increased linearly with increasing buffer concentration. The data were therefore analyzed by least-squares fitting of the simple buffer dilution expression shown in eq 1. The buffer catalytic coefficients

$$k_{\text{obs}} = k_{\text{uc}} + k_{\text{buff}}[\text{buffer}] \quad (1)$$

so obtained, k_{buff} , were separated into their general acid, k_{HA} , and general base, k_{B} , components with the aid of eq 2, in which f_{A} is the fraction of buffer present in the acidic form

$$k_{\text{buff}} = k_{\text{B}} + (k_{\text{HA}} - k_{\text{B}})f_{\text{A}} \quad (2)$$

The data (4 points) conformed to this expression well. Linear regression gave $k_{\text{HA}} = (3.08 \pm 0.05) \times 10^7 \text{ M}^{-1} \text{ s}^{-1}$ and $k_{\text{B}} = (3.3 \pm 4.4) \times 10^5 \text{ M}^{-1} \text{ s}^{-1}$, indicating that the buffer catalysis is wholly of the general acid kind (Figure S1).¹¹

Step-Scan IR Measurements. The IR spectrum of 3-diazo-3H-benzofuran-2-one (**1**) exhibits very strong bands at 2127 , 2107 , and 1767 cm^{-1} , and weaker bands at 1467 , 1401 , and 1328 cm^{-1} in CD_3CN . Some of these bands are slightly shifted in Genetron 113 (1,1,2-trichlorotrifluoroethane): 2127 , 2099 , and 1799 cm^{-1} (strong) and 1464 , 1401 , and 1328 cm^{-1} (weak).

Time-resolved IR difference spectra were generated by pulsed laser irradiation of **1** at 266 nm in CD_3CN , in wet CD_3CN (10% D_2O), and in Genetron 113. These spectra exhibited strong negative bands at the positions given above due to depletion of **1** by the laser flash. The negative bands were formed within the time resolution (50 ns) of the instrument and remained constant thereafter. In addition, a strong positive absorption band at 2050 cm^{-1} was formed within 50 ns . The decay of this band obeyed second-order kinetics, and the initial half-lives were hardly dependent on solvent or water concentration, $\tau_{1/2} \approx 50 \pm 10 \mu\text{s}$. In wet, but not in dry acetonitrile, the growth of a very weak absorption band at ca. 1816 cm^{-1} with kinetics matching that of the decay at 2050 cm^{-1} was observed. In the presence of acid ($\text{CD}_3\text{CN}/10\% \text{ D}_2\text{O}$, $1.0 \times 10^{-4} \text{ M DCIO}_4$) the decay of the 2050-cm^{-1} band was accelerated and approached a first-order rate law, $k \approx 1.8 \times 10^4 \text{ s}^{-1}$. The simultaneous growth of a band at 1818 cm^{-1} was now much more pronounced (Figure 5).

The photoproduct absorbing at 1818 cm^{-1} was still present after completion of the time-resolved experiment (30 min). It slowly disappeared within 3 d ($\tau_{1/2} \approx 1 \text{ d}$) at ambient temperature in the dark. At the same time, new absorption bands appeared at 1712 and 3540 cm^{-1} . The rate of this slow reaction is similar to that reported for the hydrolysis of 3-hydroxy-3H-benzofuran-2-one (**5**) to 2-hydroxymandelic acid (**6**), Scheme 2, in weakly acidic aqueous solutions.⁹ Thus, **5** may be identified as a major product formed by irradiation of **1** under the conditions of the step-scan experiment. The transient absorption at 2050 cm^{-1} is attributed to cumulenone **3**.⁷ For comparison,

(20) This estimate is based on the assumption that the persistent end absorbance (lower inset of Figure 3) is due to the formation of 25% isoxindigo (**7**), $\epsilon_{450} \approx 1.2 \times 10^4 \text{ M}^{-1} \text{ cm}^{-1}$.¹⁸ Similar values have been reported for related 1,2-quinone methides.

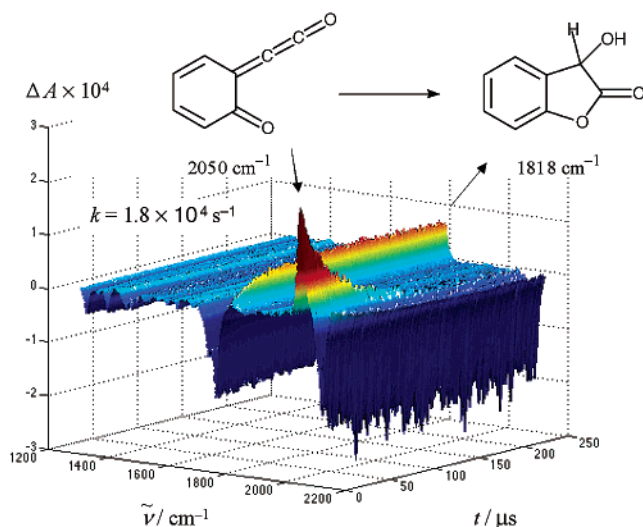


Figure 5. Temporal evolution of the IR difference spectra of **1** in CD_3CN with 10% (by vol.) D_2O and 1.0×10^{-4} M DClO_4 after excitation at 266 nm. The concentration of DClO_4 refers to the total volume.

optical LFP of **1** (excitation at 308 nm) was also done in the solvent mixture used for the step-scan measurements ($\text{CD}_3\text{CN}/10\% \text{D}_2\text{O}$, 1.0×10^{-4} M DClO_4). This gave a clean first-order decay of the 450-nm transient, $k = 5 \times 10^3 \text{ s}^{-1}$, about three times lower than the rate constant determined by the step-scan experiments. The difference may be attributed to a difference in temperature (about 22 °C in LFP, 35 °C in step-scan) and to a second-order contribution in the IR kinetics, where the transient is produced in much higher concentration (path length 0.2 mm versus 1 cm in LFP). Indeed the first half-lives of the decays in the absence and presence of 1.0×10^{-4} M DClO_4 were comparable, $\tau_{1/2} \approx 50$ and 38 μs , respectively.

Transient Raman Spectroscopy. Figure 6 presents transient resonance Raman spectra obtained for **3** in pure acetonitrile and mixed water/acetonitrile (50%/50 vol %) solvents at ~ 10 ns after 266-nm photoexcitation of **1**. Similar spectra were obtained in both solvents (indicating the same species is produced in both solvents) with strong fundamental bands observed at 1400, 1526, and 1618 cm^{-1} and weaker bands at 1150, 1241, and 2089 cm^{-1} in the water/acetonitrile solvent. The strong fundamentals at 1526 and 1618 cm^{-1} also exhibit noticeable intensity in their overtones at 3033 and 3229 cm^{-1} . This indicates these modes are strongly resonantly enhanced and the resonance Raman spectra in Figure 6 are associated with the transient absorption band observed at ~ 460 nm in the laser flash photolysis experiments. The vibrational frequencies observed in the transient resonance Raman spectra of Figure 6 are in good agreement with those computed by the DFT calculations for the cumulenone **3** (see Table 1). The DFT computed Raman intensities are also in reasonable agreement with those observed experimentally for most modes considering that the experimental spectra are resonantly enhanced, whereas the computations are an estimate for a nonresonant Raman spectrum. The differences in resonance enhancement for the Raman modes could probably account for the experimental 2089- cm^{-1} cumulenone carbonyl band being noticeably smaller than that predicted from the DFT calculations. The transient resonance Raman spectra in Figure 6 are consistent with results from the time-resolved IR experiments and further confirm the assignment of the cumulenone **3**

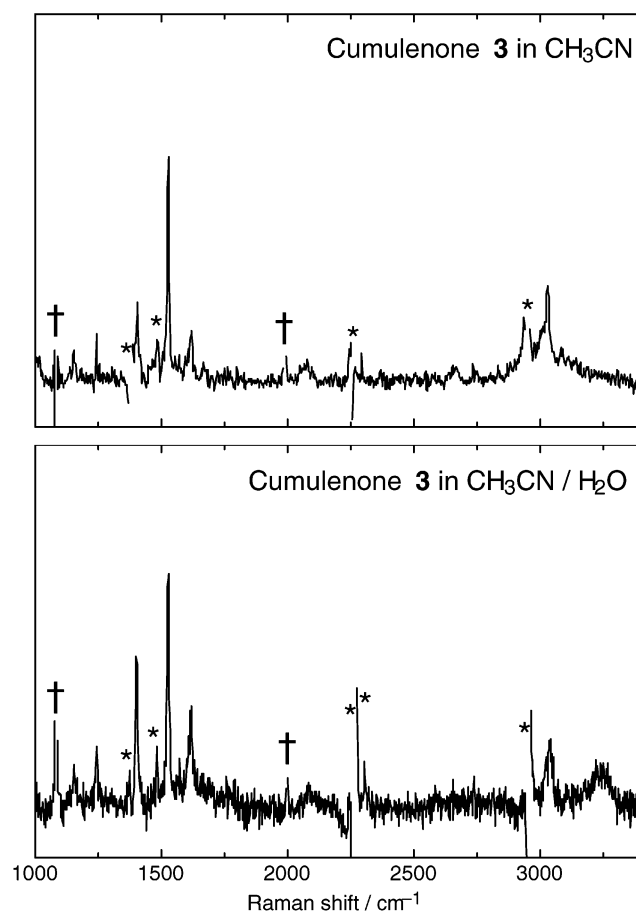


Figure 6. Transient resonance Raman spectra obtained for cumulenone **3** in acetonitrile (top) and water/acetonitrile (bottom) solvents. The numbers label the Raman shifts (in cm^{-1}) of the resonance Raman bands of **3**. The asterisks mark solvent/parent band subtraction artifacts and the daggers represent ambient/stray light features.

to the transient absorption spectra observed at 460 nm following ultraviolet excitation of **1**.

It is interesting to note that the cumulenone carbonyl Raman band upshifts noticeably from 2071 cm^{-1} in acetonitrile solvent to 2089 cm^{-1} in the water/acetonitrile solvent, whereas there are much smaller changes observed for the other Raman bands. This suggests the cumulenone carbonyl mode interacts more strongly with the aqueous solvent (presumably through some hydrogen-bonding interaction). Similar upshifts of vibrational frequencies upon changing the solvent from acetonitrile to water have been observed for the *para*-benzosemiquinone radical anion and attributed to hydrogen bonding interactions.²¹ This stronger solvent interaction for the cumulenone carbonyl mode may be a consequence of this moiety being highly reactive and susceptible to acid-catalyzed hydrolysis (Scheme 4).

Discussion

Chapman, in his study of the photolysis of 3-diazo-3H-benzofuran-2-one (**1**) under low-temperature matrix isolation conditions, was able to identify the cumulenone **3** as one of the primary products formed, both by its characteristic long-wavelength *ortho*-quinone methide-type absorption band at 460 nm and by its equally characteristic ketene carbonyl group-type

(21) Zhan, C.-G.; Chipman, D. M. *J. Phys. Chem. A* **1998**, *102*, 1230–1235.

IR band at 2040 cm^{-1} .⁷ Association of the 2040-cm^{-1} IR band and the electronic absorption at 460 nm with the same species was established by conversion of **3** to the cyclic ketene **4** ($\tilde{\nu} = 2150\text{ cm}^{-1}$) upon irradiation at long wavelengths. The frequencies obtained here by DFT calculations (2083 cm^{-1} for **3** and 2146 cm^{-1} for **4**, Table 1) are in good agreement with these assignments.

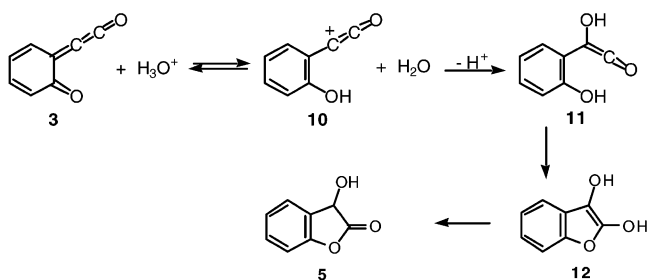
Primary Photoreaction. Pump–probe measurements (Figure 2) show formation of transient absorbance, $\lambda_{\text{max}} = 460\text{ nm}$, with a rate constant of $3.5 \times 10^{10}\text{ s}^{-1}$ after subpicosecond excitation of 3-diazo-3*H*-benzofuran-2-one (**1**). The 460-nm band agrees in shape and position with that reported for cumulenone **3** by Chapman et al., which serves to identify the present transient species as **3** and shows this substance to be a primary photoproduct of **1** in solution as well as in low-temperature matrixes. The same transient, $\lambda_{\text{max}} = 460\text{ nm}$ (Figure 3), is observed by nanosecond LFP of **1** in various solvents. The assignment of this transient is reinforced by the observation of strong transient IR absorbance at $\tilde{\nu} = 2050\text{ cm}^{-1}$ upon LFP of **1** in acetonitrile solution (Figure 5). The other IR and the Raman bands also agree well with the bands calculated for cumulenone **3** by DFT methods (Table 1).

The short-lived precursor of **3**, $\tau = 28\text{ ps}$, which exhibits diffuse absorption throughout the visible region (Figure 2), is attributed to the excited singlet state of the diazo compound, $^1\mathbf{1}^*$. If a singlet carbene, **12**, is formed by elimination of nitrogen from $^1\mathbf{1}^*$, then its lifetime must be very short, $\tau < 28\text{ ps}$. Indeed, G3 calculations indicate that ring opening of **12** to the cumulenone **3** encounters virtually no barrier. More likely, vibrational relaxation following the highly exothermic release of N_2 from $^1\mathbf{1}^*$ affords **3** directly. On the other hand, Wolff-rearrangement of $^1\mathbf{1}^*$ to the cyclic ketene **4** would require an activation energy of about 155 kJ mol^{-1} (Figure 1). Yet, Chapman et al.⁷ observed both **3** and **4** upon photolysis of **1** in an argon matrix at 12 K . As these authors have shown that **3** is converted to **4** by irradiation in the visible (Scheme 1), the formation of **4** was presumably due to secondary irradiation of the primary product **3** during photolysis of **1**.

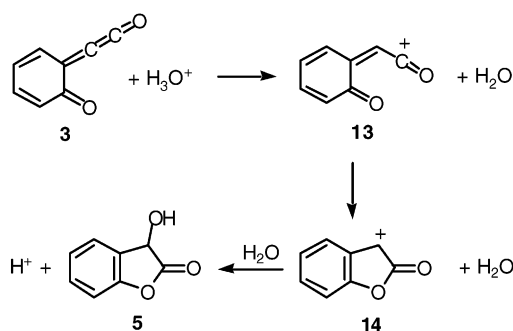
Acyclic α -carboalkoxy carbenes have triplet ground states with planar geometries and the corresponding singlet carbenes normally adopt a near-orthogonal geometry between the carbonyl and the carbene plane, allowing for overlap between the oxygen lone pair and the formally vacant p orbital at the carbene center.⁵ Given the fact that geometrical constraints force carbene **2** to be planar (Figure 1), it is remarkable that the singlet state is predicted to be the ground state of **2** at the G3 level of theory. Presumably, the singlet is stabilized relative to the triplet state due to the reduced bond angle at the carbene center.²²

Decay Kinetics of 3 in Aqueous Solution. Our product study indicates that cumulenone **3**, once formed in aqueous solution, undergoes hydration to 3-hydroxy-3*H*-benzofuran-2-one, **5**. The data displayed in Figure 4 show, moreover, that this hydration is an acid-catalyzed process. Both of the functional groups of cumulenone **3**, the quinone methide group and the ketene group, are known to undergo acid-catalyzed hydration reactions. Acid-catalyzed hydration of quinone methides occurs by rapid pre-equilibrium protonation of the quinone methide carbonyl oxygen followed by rate-determining capture of the carbenium

Scheme 3. Conceivable (but dismissed) Mechanism for Acid-Catalyzed Hydrolysis of **3**



Scheme 4. Acid-Catalyzed Hydrolysis of **3** in Aqueous Solution



ion thus formed by water.²³ In the present case, this would give the vinyl cation **10**, the reaction of which with water would give the hydroxyketene **11**, Scheme 3. This hydroxyketene could then undergo intramolecular cyclization to enol **12**, and ketonization of that would give the observed 3-hydroxy-3*H*-benzofuran-2-one product, **5**.

The solvent isotope effect observed for this reaction, $k_{\text{H}^+}/k_{\text{D}^+} = 1.74$, however, argues against this mechanism. The pre-equilibrium proton transfer that initiates the process of Scheme 3 converts a hydronium ion, whose O–H bonds are relatively loose, into a water molecule, whose O–H bonds are substantially tighter. This produces a tightening up of the isotopically substituted reactant bonds, and that generates an inverse ($k_{\text{H}}/k_{\text{D}} < 1$) isotope effect. There is both theoretical and experimental evidence for such an inverse isotope effect.²⁴ Of special relevance to the present situation are the inverse isotope effects recently found for the hydration of quinone methides, e.g., $k_{\text{H}}/k_{\text{D}} = 0.42$ for *ortho*-quinone methide²⁵ and $k_{\text{H}}/k_{\text{D}} = 0.41$ for *para*-quinone methide.²⁶ The presently determined isotope effect is, of course, not inverse, and that rules out the mechanism of Scheme 3 initiated by reaction of the cumulenone's quinone methide functional group. Consistently, we failed to detect any transient absorbance attributable to the enediol **12**, which would be expected to show similar absorbance ($\lambda_{\text{max}} \approx 280\text{ nm}$) and ketonization kinetics ($\tau \approx 1\text{ ms}$ at pH 3) as the enol of mandelic acid.^{6a}

This leaves an acid-catalyzed reaction of the cumulenone's ketene functional group. Acid-catalyzed hydration of ketenes is known to take place by rate-determining protonation of the

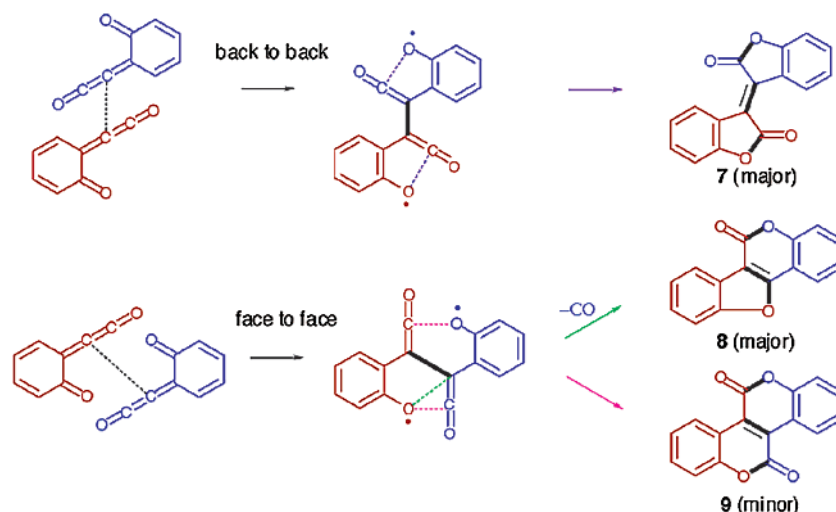
(22) Nicolaidis, A.; Matsushita, T.; Tomioka, H. *J. Org. Chem.* **1999**, *64*, 3299–3305.

(23) Chiang, Y.; Kresge, A. J.; Zhu, Y. *Pure Appl. Chem.* **2000**, *72*, 2299–2308.

(24) Kresge, A. J.; More O'Ferrall, R. A.; Powell, M. F. In *Isotopes in Organic Chemistry*; Buncl, E., Lee, C. C., Eds.; Elsevier: New York, 1987; Chapter 4.

(25) Chiang, Y.; Kresge, A. J.; Zhu, Y. *J. Am. Chem. Soc.* **2001**, *123*, 8089–8094.

(26) Chiang, Y.; Kresge, A. J.; Zhu, Y. *J. Am. Chem. Soc.* **2002**, *124*, 6349–6356.

Scheme 5. Dimerization Reactions of **3** in Aprotic Solvents

ketene on its β -carbon atom.²⁷ In the present case, this would produce the acylium ion **13**, Scheme 4, and intramolecular capture of that by the quinone methide carbonyl oxygen atom would give the carbenium ion **14**. The DFT calculations presented above for gas-phase protonation of **3**, however, indicate that structure **13** is not a metastable intermediate; *exo* addition of a proton to **3** at the β -carbon proceeds directly to **14**, which is identical with structure **d** of Chart 1, and is by far the most stable isomer of protonated **3**. Hydration of this carbenium ion would then provide the observed 3-hydroxy-3H-benzofuran-2-one product (**5**).

Because proton transfer to the cumulenone β -carbon atom is rate-determining in this reaction scheme, the hydronium ion isotope effect would contain a primary component and consequently be in the normal ($k_{\text{H}}/k_{\text{D}} > 1$) direction. Such isotope effects, however, also contain an inverse secondary component produced by tightening up of the “non-reacting” O–H bonds of the hydronium ion as they are being converted into a water molecule, which serves to reduce the magnitude of this isotope effect.²⁸ A further reduction can be expected on the basis of the very fast nature of the present reaction ($k_{\text{H}} = 7.5 \times 10^8 \text{ M}^{-1} \text{ s}^{-1}$), which will give rise to an unsymmetrical, reactant-like transition state: primary isotope effects are known to vary in magnitude with transition state symmetry, reaching maximum values for symmetrical transition states and falling off to smaller values for unsymmetrical, reactant-like or product-like transition states.²⁹ The observed isotope effect, $k_{\text{H}}^+/k_{\text{D}}^+ = 1.74$, is in fact a very reasonable value for a reaction with the present velocity occurring by the reaction mechanism of Scheme 4.

Reactions that occur by rate-determining proton transfer to the substrate, such as that in Scheme 4, should also show general acid catalysis, and such catalysis has in fact been observed for the hydration of ketenes in acidic buffer solutions.^{27b} Its occurrence here in acetic acid buffers (see Figure S1)¹¹ consequently provides further support for this reaction mech-

anism. The reaction mechanism of Scheme 3, on the other hand, might give a semblance of general acid catalysis, in a process where the buffer acid protonates cumulenone **3** on its carbonyl oxygen atom in a rapid preequilibrium step, with the buffer base then serving as a nucleophile to capture the carbenium ion **10** thus formed. In this event, the buffer base would react with the unprotonated cumulenone as well, giving a process that would appear as general base catalysis. However, no general base catalysis was observed (eq 2, Figure S1, Table S2),¹¹ and the buffer data are therefore not consistent with the reaction mechanism of Scheme 3.

The second-order rate constant for protonation of cumulenone **3** at the β -carbon, $k_{\text{H}}^+ = 7.5 \times 10^8 \text{ M}^{-1} \text{ s}^{-1}$, is, to our knowledge, the first of its kind. Its high value, 4–5 orders of magnitude higher than those of simple ketenes,²⁷ manifests the higher intrinsic reactivity of cumulenones as compared to ketenes. It should be mentioned, however, that a concerted protonation-cyclization process forming the carbenium ion **14** in a single step may be driven partly by aromatization of the quinone methide moiety.

Reactions of 3 in Aprotic Solvents. Irradiation of 3-diazo-3H-benzofuran-2-one (**1**) in acetonitrile or hexane yields a mixture of dimers (Scheme 5). Although isoxindigo (**7**) may formally be regarded as a dimer of carbene **2**, this is not the case for dibenzonaphthyrone (**8**) and coumestan (**9**). Moreover, the cumulenone **3** is formed within 50 ps of excitation of **1** in solution, and nanosecond LFP showed that its decay obeys a second-order rate law in the absence of acid (Figure 3). These findings leave no doubt that cumulenone **3**, rather than carbene **2**, is the precursor of **7–9**. The facile addition-cyclization-(elimination) reactions of **3**, $k \approx 3 \times 10^8 \text{ M}^{-1} \text{ s}^{-1}$, involve formation of a C=C double bond and two C–O bonds. No intermediates of this reaction were detected by flash photolysis or found as stationary points in the DFT calculations (B3LYP/6-31G(d)). All attempts to optimize the structures of the primary biradical intermediates shown in Scheme 5 led to one of the dimers **7** or **8**, even in the triplet state.

The high, carbene-like reactivity of cumulenone **3**, both in aqueous acid (carbon protonation, Scheme 4) and in aprotic solvents (dimerization, Scheme 5) is remarkable. Several previous publications have surmised equilibration of quinonoid

- (27) (a) Tidwell, T. T. *Ketenes*; Wiley-Interscience: New York, 1995; pp 585–587. (b) Andraos, J.; Kresge, A. J. *J. Photochem. Photobiol. A: Chem.* **1991**, *57*, 165–173. (c) Andraos, J.; Kresge, A. J.; Schepp, N. P. *Can. J. Chem.* **1995**, *73*, 539–543.
- (28) Kresge, A. J.; Sagatys, D. S.; Chen, H. L. *J. Am. Chem. Soc.* **1977**, *99*, 7228–7233.
- (29) Kresge, A. J. In *Isotope Effects on Enzyme-Catalyzed Reactions*; Cleland, W. W., O’Leary, M. H., Northup, D. B., Eds.; University Park Press: Baltimore, 1977; pp 37–63.

ketenes with a cyclic carbene isomer in an attempt to explain the formation of reaction products expected from a carbene, but Mosandl and Wentrup pointed out that the formation of such products should not be taken as unequivocal evidence for reaction via a carbene intermediate.³⁰ In the present case, reaction of **3** by preequilibration with ¹**2** is quite unlikely in view of the 54-kJ mol⁻¹ energy difference between **3** and ¹**2** calculated at the G3 level of theory. The stage at which CO is eliminated in the formation of coumestan (**8**) has not been established. Neither of the isolated dimers **7** and **9** eliminated CO upon further irradiation.

Conclusion

Cumulenone **3** is the sole primary photoproduct of 3-diazo-2-oxo-2,3-dihydrobenzofuran (**1**) in solution. High-level ab initio calculations indeed predict that ring-opening of an initially formed singlet carbene **2** is strongly favored over Wolff-rearrangement to form the cyclic ketene **4**. Isoxindigo (**7**) and coumestan (**8**) are the major products isolated after irradiation of **1** in aprotic solvents. They are formed by a remarkably facile addition-cyclization reaction of **3**, $k \approx 3 \times 10^8 \text{ M}^{-1} \text{ s}^{-1}$, in which a C=C bond and two C-O bonds appear to be formed

simultaneously. Hydrolysis of **3** in aqueous acid yielding the lactone **5** is initiated by rate-determining protonation of the cumulenone at its β -carbon atom. The rate constant of proton addition, $k_{\text{H}^+} \approx 7.5 \times 10^8 \text{ M}^{-1} \text{ s}^{-1}$, is 4–5 orders of magnitude larger than those observed for related ketenes, revealing the high intrinsic reactivity of the C₃O moiety. Thus, the chemical reactivity of cumulenone **3** mimics that expected from the singlet carbene, ¹**2**. This finding is fully consistent with ab initio calculations. The short lifetime of ¹**2** precludes any bimolecular trapping reactions, and the high energy of the singlet carbene relative to **3** excludes its participation as a pre-equilibrating intermediate in the reactions of **3**.

Acknowledgment. This work is part of Projects Nos. 20-68087.02 and 2160-064525.01 of the Swiss National Science Foundation. Financial support by Ciba Specialty Chemicals and the Natural Sciences and Engineering Research Council of Canada is gratefully acknowledged.

Supporting Information Available: Synthesis of **1**, rate data for the decay of **3** in aqueous acid and buffer solutions, and details of quantum chemical calculations. This material is available free of charge via the Internet at <http://pubs.acs.org>.

JA0365476

(30) Mosandl, T.; Wentrup, C. *J. Org. Chem.* **1993**, *58*, 747–749 and references therein.